JOC The Journal of Organic Chemistry

Article

pubs.acs.org/joc

Bioactive Nonanolide Derivatives Isolated from the Endophytic Fungus *Cytospora* sp.

Shan Lu,[†] Peng Sun,[†] Tiejun Li,[†] Tibor Kurtán,[‡] Attila Mándi,[‡] Sándor Antus,[‡] Karsten Krohn,[§] Siegfried Draeger,[∥] Barbara Schulz,[∥] Yanghua Yi,[†] Ling Li,*[,†] and Wen Zhang*[,†]

[†]Research Center for Marine Drugs, and Department of Pharmacology, School of Pharmacy, Second Military Medical University, 325 Guo-He Road, Shanghai 200433, P. R. China

[‡]Department of Organic Chemistry, University of Debrecen, POB 20, H-4010 Debrecen, Hungary

[§]Department of Chemistry, Universität Paderborn, Warburger Straße 100, 33098 Paderborn, Germany

[∥]Institut für Mikrobiologie, Technische Universität Braunschweig, Spielmannstraße 7, 31806 Braunschweig, Germany

Supporting Information

ABSTRACT: Cytospolides F–Q (**6**–**17**) and decytospolides A and B (**18** and **19**), 14 unusual nonanolide derivatives, were isolated from *Cytospora* sp., an endophytic fungus from *Ilex canariensis*. The structures were elucidated by means of detailed spectroscopic analysis, chemical interconversion, and X-ray single crystal diffraction. The solution- and solid-state conformers were compared by the combination of experimental methods (X-ray, NMR) supported by DFT calculations of the conformers. Absolute configurations were assigned using the modified Mosher's method and solution- and solid-state TDDFT ECD calculations. In an in vitro cytotoxicity assay toward the tumor cell lines of A549, HCT116, QGY, A375, and U973, the γ-lactone **17** demonstrated a potent growth inhibitory activity toward the cell line A-549, while nonanolide **16** with (2*S*) configuration showed the strongest activity against cell lines A-549, QGY, and U973. A cell cycle analysis indicated that compound **16** can significantly mediate G1 arrest in A549 tumor cells, confirming the important role of the C-2 methyl in the growth inhibition toward the tumor line. The discovery of an array of new nonanolides demonstrates the productivity of the fungus, and it is an example of chemical diversity, extending the nonanolide family by derivatives formed by ring cleavage, oxidation, esterification, and Michael addition.

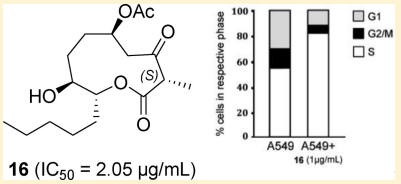

16 (IC_{50} = 2.05 μg/mL)

INTRODUCTION

Secondary metabolites belonging to the family of nonanolides (synonym decanolides) are constructed of a 10-membered macrolide core with a C-9 alkyl chain. Structurally more complex nonanolides with additional rings are sometimes also included in the family.[1] The early investigations on nonanolides can be traced back to 1942 when the first example, jasmine ketolactone, was isolated as a component of the essential oil of *Jasminum grandiflorum*.[2] The structure of this jasmine ketolactone was fully elucidated in 1964.[3] In 1975, diplodialide A was isolated as a steroid hydroxylase inhibitor from *Diplodia pinea*, representing the second report of such a structure.[4] The discovery of a series of new nonanolides from a variety of natural sources, mainly from microorganisms,[1,5−18] has continuously extended the knowledge on this group of metabolites. Nonanolides were also isolated from several marine invertebrates[1] and plants[1] and were found to have various biological activities, including cytotoxic,[1] phytotoxic,[1,5−8] antimalarial,[9] antifungal,[1,10,11] antibacterial,[1,12−14] and antimicrofilament activities,[15] as well as inhibitory effects against fish embryo larval development,[16] AChE,[17] and calmodulin-dependent cAMP phosphodiesterase.[18] The broad spectrum of bioactivity and the intriguing structure of the medium-sized ring in nonanolide analogues have drawn the attention of synthetic chemists, resulting in a great number of publications. These scientific results were subsequently summarized in several reviews,[1,19−21] followed by an increasing number of reports.[22−42] The chemistry of some nonanolides has been studied intensively, and their total synthesis was reported repeatedly. Some examples include the cholesterol biosynthesis inhibitor decarestrictine,[1,19,20,22−25] the antimicrofilament agent microcarpalide,[1,19,21] the phytotoxin herbarumins,[1,19,21,23,26−30] and the bacterial DNA primase inhibitor Sch 642305.[1,19,21,31]

During our ongoing screening for biologically active secondary metabolites from fungi,[43−46] we recently investigated *Cytospora* sp., an endophytic fungus from *Ilex canariensis* (Aquifoliaceae, Aquifoliales), an evergreen shrub from the island of Gomera, Spain. The fungus was cultivated on biomalt agar medium. The crude extract of the culture showed pronounced antifungal activity against *Microbotryum violaceum* and moderate algicidal activity against *Chlorella fusca*. Preliminary investigation of the crude acetone extract in our laboratory led to the isolation and structural elucidation of five novel 10-membered macrolides, cytospolides A–E (**1**–**5**).[46] The skeleton of cytospolides A–E (**1**–**5**) was constructed of 15 carbons and extended the nonanolide family by a novel carbon

Received: August 23, 2011
Published: October 19, 2011

   dx.doi.org/10.1021/jo201755v | *J. Org. Chem.* 2011, 76, 9699–9710

skeleton with a unique structural feature of a C-2 methyl group. Both C-2 epimers were isolated from the same fungal extract, and the epimers differed considerably in their cytotoxic activities against the A549 cell line.[46] Our investigation on the trace compounds of the crude extract has now resulted in the isolation of additional new members of this family, namely the cytospolides F−Q (**6**−**17**) and decytospolides A and B (**18** and **19**). Compounds **6**−**12** and **16** are analogues of cytospolides A−D (**1**−**4**) and cytospolide E (**5**), respectively. The cyclization products **13**−**15** and rearrangement products **17** are furan containing lactones, while the lipid ketones **18** and **19** are decarboxylated derivatives of cytospolides. Herein, we report the isolation, structural elucidation, including relative and absolute configuration, and bioactivities of these compounds.

RESULTS AND DISCUSSION

The fungus *Cytospora* sp. was cultivated on biomalt agar medium for 4 weeks and then extracted with acetone. The crude extract was fractionated on a silica gel column, followed by Sephadex LH-20 column chromatography and RP-HPLC, to yield pure cytospolides F−Q (**6**−**17**) and decytospolides A and B (**18** and **19**). Structures of these metabolites were elucidated by a combination of detailed spectroscopic analysis, chemical interconversion, X-ray single crystal diffraction, and comparison with data of reported cytospolides A−E (**1**−**5**).[46] The absolute configurations were determined by the modified Mosher's method and TDDFT calculations of ECD spectra, including the solid-state TDDFT ECD approach.

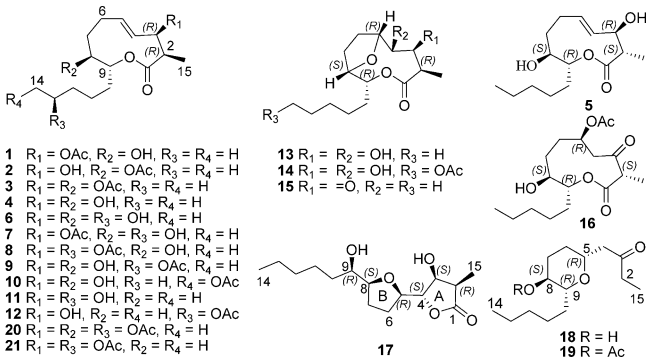

Cytospolide F (**6**) was obtained as an optically active colorless oil. Its molecular formula $C_{15}H_{26}O_5$ was established by HRESIMS, indicating an additional oxygen atom in comparison to that of **4**. The ^{1}H and ^{13}C NMR spectra of **6** showed signals identical to those of **4** in the 10-membered lactone ring, except for the signals of the side chain, in which a hydroxyl group was introduced at C-13 (Tables 1 and 2). The location of 13-OH was deduced by the doublet signal of H_3-14 and confirmed by the correlations from H_3-14 to H_3-15 established by the ^{1}H−^{1}H COSY and HMBC spectra. The NOESY spectrum of **6** suggested the same relative configuration of the 10-membered lactone ring as that of **4**. Similarly to the ECD spectrum of **4**,[46] the ECD spectrum of **6** showed a negative Cotton effect (CE) at 195 nm, indicating the same (2*R*) absolute configuration. On the basis of the relative configuration, the absolute configuration of the lactone ring of **6** was then assigned as (2*R*,3*R*,8*S*,9*R*).

In order to determine the absolute configuration of the secondary C-13 hydroxyl group by the Mosher's method,[47−49] diastereomeric triesters were prepared with (*R*)- and (*S*)-MTPA. As shown in Figure 1, the positive and negative $\Delta\delta$ (δ_S−δ_R) values for the protons flanking the C-8 chirality center suggested (8*S*) absolute configuration in accordance with the CD result. In contrast, protons flanking the C-13 chirality center showed positive $\Delta\delta$ (δ_S − δ_R) values at both sides making the assignment ambiguous, which is presumably due to the presence of the C-8 MTPA ester group. However, 14-H had much smaller positive value (+15.4) than 10−12-H (+112.5, +141.7, +58.8, respectively), which is most likely governed by the C-13 MTPA ester group and suggested (13*S*) absolute configuration (Figure 1). The chemical shift difference data of MTPA diester and monoester derivatives of related derivatives **11** and **18** corroborate well our assignation (vide infra). The absolute configuration of compound **6** was thus elucidated as (−)-(2*R*,3*R*,8*S*,9*R*,13*S*)-**6**.

Cytospolide G (**7**), an optically active colorless oil, had the molecular formula $C_{17}H_{28}O_6$ as deduced from HRESIMS. The ^{1}H and ^{13}C NMR spectra of **7** (Tables 1 and 2) resembled those of **6**, revealing their similar structures. The presence of signals at δ_H = 2.14, δ_C = 170.4, and 20.9 in combination with the typical downfield shift of H-3 from 4.30 in **6** to 5.34 in **7** indicated the presence of an acetyl group at C-3. Detailed 2D NMR analysis, including HSQC, HMBC, ^{1}H−^{1}H COSY, and NOESY, supported the above conclusion. Acetylation of **6** and **7** gave the triacetyl derivative **20** with identical data in all respects, including MS, NMR, and $[\alpha]^{20}_D$ (Experimental section). The structure and absolute stereochemistry of **7** was thus determined as the 3-acetyl derivative of **6** with the (−)-(2*R*,3*R*,8*S*,9*R*,13*S*) absolute configuration.

Cytospolide H (**8**) was isolated as an optically active colorless oil. Its molecular formula $C_{19}H_{30}O_7$ was established by HRESIMS. Again, the ^{1}H and ^{13}C NMR spectra of **8** (Tables 1 and 2) showed similarity to those of **7** with the exception of an additional acetyl group (δ_H = 2.03, δ_C = 170.8, and 21.4). The location of the acetyl group at C-13 was shown by the typical downfield shift of the proton signal at C-13 from 3.80 in **7** to 4.89 in **8** (Tables 1 and 2). Acetylation of **8** resulted in the same product (**20**) (Experimental Section) as that of **6** and **7**. The structure of **8** was then determined as shown above with (−)-(2*R*,3*R*,8*S*,9*R*,13*S*) absolute configuration.

Cytospolides I (**9**) and J (**10**) were isolated as a 7:3 mixture that could not be separated using normal-phase column chromatography or reversed-phase HPLC techniques. However, the structural elucidation of both compounds from the mixture was possible because of the well-separated resonance signals observed in their ^{1}H and ^{13}C NMR spectra (Tables 1 and 2). Compounds **9** and **10** had the same molecular formula of $C_{17}H_{28}O_6$ as established by ESIMS, ^{13}C NMR, and DEPT spectra. The ^{1}H and ^{13}C NMR spectra of both compounds showed patterns similar to that of **6** in the 10-membered lactone ring. Differences were only recognized in the substituent pattern of an acetoxyl group at the side chain. The position of the acetoxy group in **9** was obviously the same as that in **8** due to their identical ^{13}C NMR data from C-10 to C-15 (Table 2). In the ^{1}H and ^{13}C NMR spectra of **10**, the appearance of a primary oxygenated carbon (δ_H = 4.06, t, J = 6.7; δ_C = 64.4, t) and a lack of the 14-methyl signals led the location of the acetoxyl group at C-14. The established structures were fully supported by 2D NMR experiments.

Cytospolide K (**11**) was also obtained as an optically active colorless oil, with the molecular formula of $C_{15}H_{26}O_4$, as deduced from HRESIMS. The ^{1}H and ^{13}C NMR spectra of **11** were closely related to those of **6**, except that the secondary alcohol at C-8 (δ_H = 3.65, δ_C = 73.6/73.8) in **6** was replaced by

dx.doi.org/10.1021/jo201755v | J. Org. Chem. 2011, 76, 9699−9710

Table 1. ^{1}H NMR Data for Cytospolides F–J (6–10)[a]

no.	6	7	8	9	10
2	2.68, qd, 6.9, 3.1	2.73, qd, 7.2, 3.6	2.73, qd, 7.0, 3.1	2.70, qd, 7.0, 3.0	2.70, qd, 7.0, 3.0
3	4.30, brs	5.34, brs	5.34, brs	4.32, brs	4.32, brs
4	5.60, ov	5.59, dd, 16.2, 2.4	5.59, d, 16.1	5.62, ov	5.62, ov
5	5.60, ov	5.52, ddd, 16.2, 9.6, 4.2	5.55, ddd, 16.1, 9.2, 4.3	5.62, ov	5.62, ov
6α	2.14, m	2.09, m	2.11, m	2.16, m	2.16, m
6β	2.39, m	2.35, m	2.36, m	2.40, m	2.40, m
7α	1.99, m	1.97, m	1.98, m	2.00, m	2.00, m
7β	1.83, m	1.79, m	1.83, m	1.85, m	1.85, m
8	3.65, t, 7.3	3.64, t, 7.2	3.62, m	3.65, t, 7.0	3.65, t, 7.0
9	4.76, m	4.76, dt, 7.2, 3.6	4.75, dt, 7.2, 3.6	4.77, dt, 7.2, 3.6	4.77, dt, 7.2, 3.6
10a	1.81, m	1.78, m	1.55, m	1.73, m	1.75, m
10b	1.63, m	1.60, m	1.55, m	1.55, m	1.75, m
11a	1.42, m	2.07, m	1.33, m	1.30, m	1.32, m
11b	1.42, m	2.01, m	1.33, m	1.30, m	1.32, m
12a	1.45, m	1.45, m	1.55, m	1.45, m	1.33, m
12b	1.45, m	1.40, m	1.55, m	1.45, m	1.33, m
13a	3.80, m	3.80, m	4.89, m	4.91, m	1.62, m
13b					1.62, m
14	1.18, d, 6.0	1.18, d, 6.1	1.19, d, 6.2	1.21, d, 6.2	4.06, t, 6.7
15	1.28, d, 7.0	1.17, d, 7.0	1.18, d, 7.0	1.30, d, 7.0	1.30, d, 7.0
3-OAc		2.14, s	2.14, s		
13-OAc			2.03, s	2.04, s	
14-OAc					2.06, s

[a]In $CDCl_3$, assignments made by DEPT, ^{1}H–^{1}H COSY, HSQC, HMBC, and NOESY.

a methylene single (δ_H = 1.50 and 1.81; δ_C = 33.5) in **11** (Table 3). Analysis of the ^{1}H–^{1}H COSY and HMBC spectra of **11** supported the proposed planar structure. On the basis of the corresponding chirality centers of the lactone ring, the NOESY experiment suggested that **11** has the same relative configuration as **6**. The ECD curve of **11** had a negative CE at 195 nm in agreement with those of **4** and **6** indicating the same (2*R*) absolute configuration. The absolute configuration of the three chirality centers of the lactone ring was thus assigned as (2*R*,3*R*,9*S*).

The absolute configuration of C-13 was determined by the modified Mosher's method.[47−49] The negative $\Delta\delta$ ($\delta_S - \delta_R$) value of H-14 and the positive ones of H-8–H-12 allowed determination of the absolute configuration at C-13 as (13*S*) (see the Supporting Information, Figure S1). Moreover, the negative $\Delta\delta$ ($\delta_S - \delta_R$) value of 15-H and the positive ones of H-4–H_2-6 corroborated the absolute configuration determined by ECD. The absolute configuration of compound **11** was thus elucidated unambiguously as (−)-(2*R*,3*R*,9*S*,13*S*)-**11**.

Cytospolide L (**12**) was isolated as an optically active colorless oil with its molecular formula of $C_{17}H_{28}O_5$ being established by HRESIMS. The ^{1}H and ^{13}C NMR spectra of **12** displayed a great similarity to those of **11**, except for the presence of an additional acetyl group (δ_H = 2.02, s; δ_C = 170.8, s and 21.4, q) (Table 3). The location of the acetyl group at C-13 was assured by the downfield shift of the H-13 (δ_H = 4.87 in **12** and 3.78 in **11**), so that compound **12** was determined as the 13-acetyl derivative of **11**. The long-range correlation from H-13 to the acetyl carbonyl atom (δ_C = 170.8) in the HMBC spectrum further confirmed the proposed structure. Acetylation of **11** and **12** resulted in the same product **21** (Experimental Section). The absolute stereochemistry of compound **12** was thus determined to be the same as that of **11**.

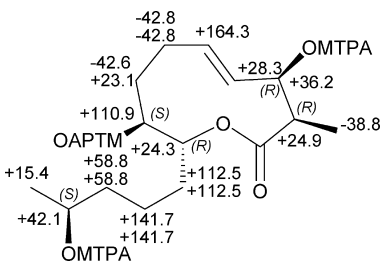

Figure 1. $\Delta\delta$ (δ_S-δ_R) values (in Hz) for the MTPA esters of **6**.

Interestingly, carbon atoms of C-8, C-12, C-13, and C-14 of compounds **6–9** were observed to resonate as two signals when at least one of the C-8 and C-13 carbons has a free hydroxyl group. The two series of signals may be due to two different intramolecular hydrogen-bonding interactions. These duplicated signals change into single ones when intramolecular hydrogen bonds are broken, i.e., if one of the oxygenated groups at C-8 and C-13 was absent (e.g., in **1–5**[46] and **10–12** see Table 2) or none of the C-8 and C-13 substituents was a free hydroxyl group (e.g., acetylating **6–8** to **20**).

Cytospolide M (**13**) was isolated as optically active colorless crystals. The HRESIMS of **13** established the molecular formula $C_{15}H_{26}O_5$, indicating three double bond equivalents. The IR absorption showed the presence of hydroxy (3346 cm^{-1}) and ester carbonyl (1731 cm^{-1}) groups. The ^{13}C NMR and DEPT spectra revealed one sp^2 carbon of an ester carbonyl atom at lower field and fourteen sp^3 carbons (1 × CH, 6 × CH_2, 2 × CH_3, and 5 × OCH at higher field, which were assigned to their corresponding proton signals by HSQC experiments (Table 4). Obviously, there are two rings present in the structure based on the established molecular formula and the relevant NMR data.

The planar structure and (2*R**,3*S**,4*R**,5*R**,8*S**,9*R**) relative stereochemistry of **13** were determined by both NMR (Figure 2 and 3) and single-crystal X-ray analysis (Figure 4), the geometry of the latter was then used to determine the absolute

dx.doi.org/10.1021/jo201755v | J. Org. Chem. 2011, 76, 9699–9710

Table 2. ^{13}C NMR Data for Cytospolides F–J (6–10)[a]

no.	6	7	8	9	10
1	174.3/174.4, C	172.4, C	172.3, C	174.3, C	174.4, C
2	46.7, CH	44.9/45.0, CH	45.0, CH	46.7, CH	46.7, CH
3	72.0 CH	72.5/72.6, CH	72.5, CH	72.0, CH	72.0, CH
4	133.2, CH	128.9, CH	128.9, CH	133.2, CH	133.2, CH
5	127.5, CH	129.5, CH	129.6, CH	127.5, CH	127.5, CH
6	28.6/28.9, CH_2	29.4, CH_2	29.3, CH_2	28.4, CH_2	28.5, CH_2
7	38.6, CH_2	38.8, CH_2	38.6, CH_2	38.5, CH_2	38.6, CH_2
8	73.6/73.8, CH	73.6/73.8, CH	73.6/73.9, CH	73.6/73.8, CH	73.4, CH
9	77.6, CH	77.4/77.5, CH	77.3, CH	77.4, CH	77.6, CH
10	31.5/32.1, CH_2	32.1, CH_2	32.0, CH_2	32.0, CH_2	32.1, CH_2
11	20.3/20.8, CH_2	20.7, CH_2	20.2/20.6, CH_2	20.2/20.6, CH_2	24.3, CH_2
12	38.8/38.9, CH_2	38.5/38.6, CH_2	35.7/35.8, CH_2	35.7/35.8, CH_2	25.9, CH_2
13	67.5/68.0, CH	67.5/68.1, CH	70.6/70.8, CH	70.6/70.7, CH	31.7, CH_2
14	23.5/23.6, CH_3	23.5/23.7, CH_3	19.9/20.1, CH_3	19.9/20.1, CH_3	64.4, CH_2
15	12.5, CH_3	12.2, CH_3	12.2, CH_3	12.4, CH_3	12.4, CH_3
3-OAc		170.4, C	170.4, C		
		20.9, CH_3	20.9, CH_3		
13-OAc			170.8, C	170.8/170.9, C	
			21.4, CH_3	21.4, CH_3	
14-OAc					171.3, C
					21.0, CH_3

[a]In $CDCl_3$, assignments made by DEPT, $^1H–^1H$ COSY, HSQC, and HMBC.

Table 3. NMR Data for Cytospolides K and L (11 and 12)[a]

	11		12	
no.	δ_H, m, J (Hz)	δ_C, m	δ_H, m, J (Hz)	δ_C, m
1		174.4, C		174.3, C
2	2.69, qd, 6.9, 3.1	47.1, CH	2.68, qd, 6.8, 3.3	47.1, CH
3	4.30, brs	72.8, CH	4.31, brs	72.8, CH
4	5.62, d, 17.4	133.4, CH	5.62, d, 17.5	133.4, CH
5	5.57 (ddd, 17.4, 9.5, 3.7)	127.3, CH	5.57, ddd (17.5, 9.0, 3.0)	127.4, CH
6α	1.95, m	32.7, CH_2	1.95, m	32.6, CH_2
6β	2.30, m		2.30, m	
7α	1.84, m	28.1, CH_2	1.84, m	28.0, CH_2
7β	1.45, m		1.44, m	
8α	1.50, m	33.5, CH_2	1.47, m	33.4, CH_2
8β	1.81, m		1.78, m	
9	4.75, q, 6.0	76.2, CH	4.74, q, 6.0	76.0, CH
10a	1.55, m	35.8, CH_2	1.55, m	35.5, CH_2
10b	1.45, m		1.47, m	
11a	1.40, m	21.5, CH_2	1.31, m	21.1, CH_2
11b	1.40, m		1.31, m	
12a	1.45, m	38.9, CH_2	1.55, m	35.6, CH_2
12b	1.45, m		1.55, m	
13	3.78, m	67.9, CH	4.87, m	70.7, CH
14	1.18, d, 6.1	23.6, CH_3	1.19, d, 6.5	19.9, CH_3
15	1.28, d, 7.0	12.5, CH_3	1.28, d, 7.0	12.5, CH_3
13-OAc			2.02, s	170.8, C
				21.4, CH_3

[a]In $CDCl_3$, assignments made by DEPT, $^1H–^1H$ COSY, HSQC, HMBC, and NOESY.

configuration of **13** by the solid-state TDDFT ECD approach.[50] In this method, the DFT-optimized X-ray structure is used as input for TDDFT ECD calculations,[51,52] and the resultant computed ECD spectrum is compared with the experimental solid-state ECD measured as a KCl disk (Figure 5). The solution- and solid-state ECD spectra of **13** showed a negative band at 214 nm and a positive one below 200 nm. Their good agreement suggested that the solid-state X-ray conformer is also prevalent in solution. This was confirmed by a conformational analysis on the truncated 9-methyl model compound of **13**, which showed that the solid-state conformer had 94.8% population (see the Supporting Information, Figure S2). The ECD spectra calculated for the optimized (2*R*,3*S*,4*R*,5*R*,8*S*,9*R*) enantiomer of the X-ray structure reproduced well the experimental solid-state ECD, allowing the determination of absolute configuration.

dx.doi.org/10.1021/jo201755v | J. Org. Chem. 2011, 76, 9699–9710

Table 4. NMR Data for Cytospolides M, N, and Q (13, 14, and 17)[a]

	13		14		17	
	δ_H, m, J (Hz)	δ_C, m	δ_H, m, J (Hz)	δ_C, m	δ_H, m, J (Hz)	δ_C, m
1		175.1, C		175.3, C		177.9, C
2	2.75, qd, 6.9, 2.5	45.6, CH	2.75, qd, 7.0, 2.3	45.5, CH	2.80, m, 7.4	39.2, CH
3	3.88, brs	81.9, CH	3.88, brs	81.8, CH	4.51, dd, 7.0, 3.6	71.1, CH
4	3.55, d, 9.1	76.5, CH	3.53, t, 7.2	76.4, CH	4.12, dd, 8.0, 3.6	85.2, CH
5	4.10, dd, 9.1, 7.0	80.6, CH	4.10, dd, 8.4, 7.2	80.6, CH	3.94, dt, 7.5, 4.0	78.5, CH
6α	2.08, m	29.5, CH_2	2.08, m	29.5, CH_2	2.09, m	28.9, CH_2
6β	2.00, m		2.00, m		1.95, m	
7α	1.87, m	23.4, CH_2	1.86, m	23.5, CH_2	1.83, m	23.1, CH_2
7β	1.84, m		1.84, m		1.94, m	
8	4.03, dt, 8.3, 3.8	81.2, CH	4.02, dt, 7.9, 3.8	81.1, CH	3.90, dt, 8.0, 3.0	83.4, CH
9	5.36, dt, 9.1, 3.8	75.0, CH	5.34, br d, 8.8	74.9, CH	3.82, dt, 7.8, 3.6	71.5, CH
10a	1.54, m	29.1, CH_2	1.54, m	28.9, CH_2	1.38, m	33.1, CH_2
10b	1.45, m		1.45, m		1.38, m	
11a	1.35, m	25.6, CH_2	1.43, m	25.6, CH_2	1.50, m	25.6, CH_2
11b	1.35, m		1.43, m		1.33, m	
12a	1.32, m	31.6, CH_2	1.43, m	25.7, CH_2	1.30, m	31.8, CH_2
12b	1.32, m		1.43, m		1.30, m	
13a	1.31, m	22.4, CH_2	1.64, m	28.4, CH_2	1.32, m	22.6, CH_2
13b	1.31, m		1.64, m		1.32, m	
14	0.90, t, 6.6	14.0, CH_3	4.06, t, 6.8	64.3, CH_2	0.90, t, 6.5	14.0, CH_3
15	1.30, d, 6.9	14.6, CH_3	1.29, d, 6.9	14.6, CH_3	1.27, d,7.5	8.8, CH_3
14-OAc			2.04, s	171.2, C		
				21.0, CH_3		

[a]In $CDCl_3$, assignments made by DEPT, $^1H-^1H$ COSY, HSQC, HMBC, and NOESY.

Cytospolide N (**14**) was isolated as an optically active colorless gum. Its molecular formula $C_{17}H_{28}O_7$ was established by HRESIMS. The ^1H and ^{13}C NMR spectra of **14** (Table 4) were almost identical to those of **13**, except for replacement of signals for the 14-methyl group (δ_C = 14.0; δ_H = 0.9) in **13** by signals of an oxygenated methylene group (δ_C = 64.3; δ_H = 4.06) in **14**. Moreover, signals of an acetyl group (δ_C 171.2, 21.0 and δ_H 2.04) indicated that compound **14** is the 14-acetoxy derivative of **13**. A detailed 2D NMR analysis, including $^1H-^1H$ COSY, HMBC, and NOESY, supported the established structure and relative configuration. The absolute configuration at C-2 of **14** was proven to be the same as that of **13** by its ECD spectrum, showing a similar negative band above 200 nm, which afforded the absolute configuration as (2*R*,3*S*,4*R*,5*R*,8*S*,9*R*)-**14**.

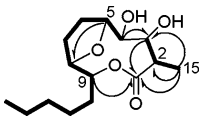

Figure 2. $^1H-^1H$ COSY (bond) and selected HMBC (arrow) correlations of **13**.

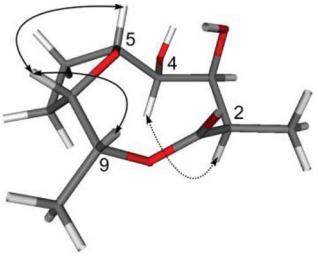

Figure 3. Key NOESY correlations of **13** indicated on the lowest energy DFT solution conformer of the truncated 9-methyl derivative.

Cytospolide O (**15**), an optically active colorless oil, has the molecular formula $C_{15}H_{24}O_4$ as deduced from HRESIMS. A comparison of the ^1H and ^{13}C NMR spectra of **15** with those of **13** revealed similarity. However, the 3-OH and 4-OH groups of **13** were replaced by a carbonyl oxygen and a proton, respectively (Table 5). The C-4 methylene group was assigned by the proton spin system from H_2-4 to H_3-14 as deduced from the $^1H-^1H$ COSY spectrum (Figure 6). The C-3 ketone carbonyl group was confirmed by the observation of long-range correlation of both H-2 and H_3-15 with C-1 and C-3, H-4 with C-2 and C-3 in the HMBC spectrum. The diagnostic NOE cross peaks between H-4α and H-2, H-6α, and H-7α, and between H-7α and H-10b indicated an α configuration of these protons, and H-6β, H-8 and H-9 were therefore identified as β protons. The observed NOE effects between H-8 and both H-6β and H-9 supported the established (2*R**,5*R**,8*S**,9*R**)

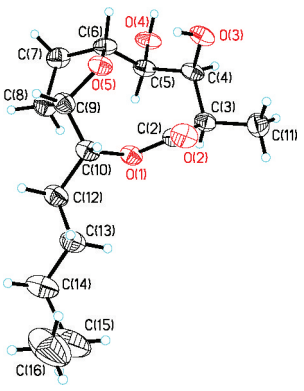

Figure 4. Single-crystal X-ray structure of **13** (ORTEP drawing).

dx.doi.org/10.1021/jo201755v | J. Org. Chem. 2011, 76, 9699–9710

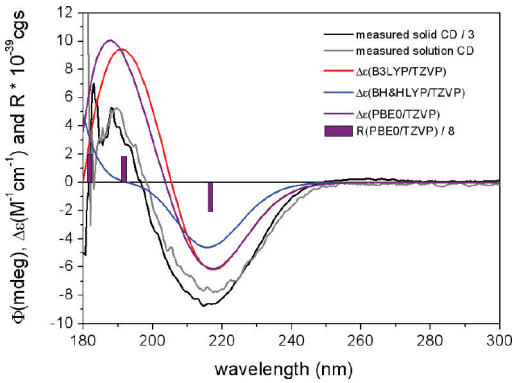

Figure 5. Experimental solution (MeCN) and solid-state (KCl) ECD spectra of cytospolide M (**13**) compared with the TDDFT ECD spectra calculated for the optimized X-ray geometry of the (2*R*,3*S*,4*R*,5*R*,8*S*,9*R*) enantiomer of **13**. Bars represent the calculated rotatory strength (*R*) obtained with the PBE0/TZVP method.

Table 5. NMR Data for Cytospolides O and P (15 and 16)[a]

	15		16	
no.	δ_H, m, *J* (Hz)	δ_C, m	δ_H, m, *J* (Hz)	δ_C, m
1		170.6, C		170.3, C
2	3.73, q, 6.7	57.2, CH	3.46, q, 7.0	55.7, CH
3		203.6, C		201.2, C
4*α*	3.14, dd, 11.7, 4.4	47.1, CH_2	2.59, dd, 15.0, 5.3	41.8, CH_2
4*β*	2.34, t, 11.4		3.13, dd, 15.0, 11.0	
5	4.56, m	77.2, CH	5.38, m	69.9, CH
6*α*	1.78, m	30.9, CH_2	2.05, m	26.8, CH_2
6*β*	2.00, m		1.38, m	
7*α*	2.10, m	24.0, CH_2	1.64, m	28.8, CH_2
7*β*	1.93, m		1.65, m	
8	4.07, dt, 7.0, 3.8	80.8, CH	3.55, br t, 8.8	73.5, CH
9	5.33, dt, 9.6, 3.6	75.9, CH	4.89, dt, 8.5, 3.0	79.4, CH
10a	1.60, m	29.2, CH_2	1.83, m	32.7, CH_2
10b	1.47, m		1.57, m	
11a	1.47, m	25.6, CH_2	1.28, m	24.5, CH_2
11b	1.38, m		1.28, m	
12a	1.33, m	31.6, CH_2	1.28, m	31.5, CH_2
12b	1.33, m		1.28, m	
13a	1.30, m	22.5, CH_2	1.28, m	22.4, CH_2
13b	1.30, m		1.28, m	
14	0.90, t, 7.0	14.0, CH_3	0.88, t, 6.8	13.9, CH_3
15	1.26, d, 6.7	10.4, CH_3	1.33, d, 7.0	11.2, CH_3
5-OAc			2.01, s	170.1, C
				21.1, CH_3

[a]In $CDCl_3$, assignments made by DEPT, $^1H-^1H$ COSY, HSQC, HMBC, and NOESY.

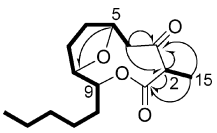

Figure 6. $^1H-^1H$ COSY (bond) and selected HMBC (arrow) correlations of **15**.

relative stereochemistry (see the Supporting Information, Figure S3).

For the configurational assignment of **15**, the solution TDDFT ECD protocol was pursued. The solution ECD spectra of **15** showed a positive n→*π** band around 300 nm and a negative band below 250 nm. The conformational analysis of the truncated C-9 methyl derivative of **15** afforded three conformers with 79.0%, 17.1% and 3.9% populations (see Supporting Information, Figure S4). In the two high-energy conformers, the C-3 carbonyl group was rotated compared to that of the lowest-energy one. The ECD spectrum calculated for the (2*R*,5*R*,8*S*,9*R*) enantiomer of the solution conformers of truncated **15** reproduced well the experimental solution ECD (see Supporting Information, Figure S5) curve of **15**, allowing determination of the absolute configuration as (2*R*,5*R*,8*S*,9*R*).

Cytospolide P (**16**) was obtained as an optically active colorless crystal. The HRESIMS showed the molecular formula of $C_{17}H_{28}O_6$, indicating four double bond equivalents. The presence of a ketone and two ester functionalities in the molecule was deduced from the IR absorption (1736, 1708 cm^{-1}) and the ^{13}C NMR and DEPT spectra (δ_C = 201.2, 170.1, and 170.3) (Table 5), accounting for three degrees of unsaturation. The remaining double bond equivalent was attributed to the presence of the lactone ring. The detailed NMR (Figures 7 and S6) and single crystal X-ray diffraction

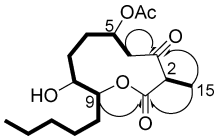

Figure 7. $^1H-^1H$ COSY (bond) and selected HMBC (arrow) correlations of **16**.

(Figure 8) analysis of cytospolide P (**16**) afforded its planar structure and (2*S**,5*R**,8*S**,9*R**) relative configuration.

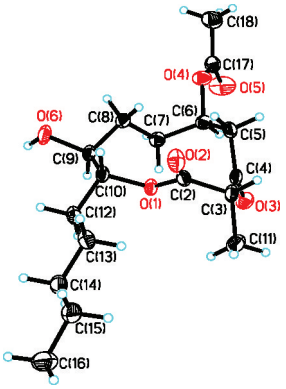

Figure 8. Single-crystal X-ray structure of **16** (ORTEP drawing).

Although **15** and **16** had the same *β*-keto lactone chromophore, the characteristic n→*π** CE of **16** was negative (Δ*ε* = −0.88 at 290 nm), opposite to that of **15** (Δ*ε* = +1.14 at 296 nm), while their ECD bands above 200 nm (lactone n→*π**) exhibited the same positive sign. For the configurational assignment of **16**, the TDDFT ECD spectra were calculated for the optimized (2*S*,5*R*,8*S*,9*R*) enantiomer of the X-ray geometry. Based on the good agreement with the experimental solid-state ECD measured as KCl disk, the absolute configuration was deduced as (2*S*,5*R*,8*S*,9*R*). Thus, **16** has an opposite absolute configuration at C-2 compared to that of **15**, which was responsible for the opposite CE of the ketone n→*π** ECD transition. A conformational analysis of **16** was also performed on a truncated C-9 methyl model compound, which showed

dx.doi.org/10.1021/jo201755v | *J. Org. Chem.* 2011, 76, 9699–9710

that the solid-state conformer with equatorial 8-OH is the most abundant conformer represented by six slightly different conformers with a total population of 58.3% (see the Supporting Information, Figure S7). The 8-OH_{ax} conformer was represented by four conformers with 38.4% of the total population. In accordance with the result of the conformational analysis, the measured solution and solid-state ECD spectra were quite similar (see the Supporting Information, Figure S8).

Cytospolide Q (**17**) was isolated as an optically active colorless gum. Its molecular formula $C_{15}H_{26}O_5$ was established by HRESIMS. The IR absorption showed absorptions of a hydroxy (3435 cm^{-1}) and an ester carbonyl (1768 cm^{-1}) group. This was in agreement with the observation of an ester carbonyl and fourteen sp^3 carbons (1 × CH, 6 × CH_2, 2 × CH_3, and 5 × OCH) in the ^{13}C NMR and DEPT spectra (Table 4). Three degrees of double bond equivalence were attributed to one carbonyl group and two rings in the molecule. The proton spin system from H_3-15 to H_3-14 was readily identified by $^1H-^1H$ COSY, and the planar structure was then established by the HMBC correlations as shown in Figure 9.

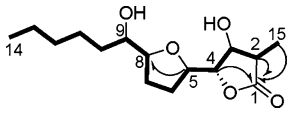

Figure 9. $^1H-^1H$ COSY (bond) and selected HMBC (arrow) correlations of **17**.

The relative stereochemistry of **17** was elucidated on the basis of detailed analysis on its NOE data. Concerning the lactone ring (A), the NOE effect between H-4 and H_3-15 indicated a β configuration of the protons while the NOE effect between H-3 and H-5 indicated their α orientation. As for the tetrahydrofuran ring (B), the observed NOE effects between H-4 and H-7β, and between H-5 and H-8 led to the assignment of H-7β as a β proton and H-5 and H-8 as α protons, respectively. Ring A is attached to ring B in a β position (see the Supporting Information, Figure S9). The relative configuration of H-9 was deduced from the homo- and heteronuclear ^3J couplings.[53] The small coupling constant of $^3J_{H8,H9}$ = 3.0 Hz indicated a gauche arrangement of H-8 and H-9, and the large coupling constant of $^3J_{C7,H9}$ = 11.5 Hz, measured by means of *J*-modulated HMBC experiments,[54] indicated antiperiplanar orientation of C-7 and H-9, which finally led to (2*R**,3*S**,4*S**,5*R**,8*S**,9*R**) relative configuration.

A conformational analysis of the solution conformers of truncated **17** confirmed the NMR coupling pattern. In the lowest-energy conformer (67.7% population) the $\omega_{C7,C8,C9,H9}$ torsional angle was 174.2°, while the $\omega_{H8,C8,C9,H9}$ was found to be −60.7°, corroborating the values of experimental homonuclear and heteronuclear coupling constants (see the Supporting Information, Figure S10). These torsional angles have similar values in the higher-energy conformers as well, since they only differed in the orientation of their OH groups. The 9-OH was hydrogen-bonded to the oxygen of the 3-OH in conformer A, B, D with 67.7%, 12.8%, and 5.6% populations, respectively, and the 3-OH was hydrogen-bonded to the oxygen of 9-OH in two minor conformers with 8.4% and 2.3% populations.

The structure and relative stereochemistry of **17** were further confirmed by a single-crystal X-ray analysis (Figure 10). The X-ray diffraction also established the absolute stereochemistry

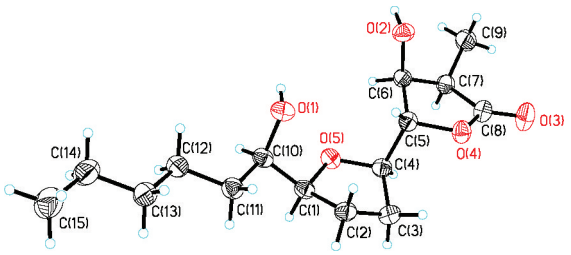

Figure 10. Single-crystal X-ray structure of **17** (ORTEP drawing).

of **17** as depicted in Figure 10 with the convincing absolute structure parameter 0.1 (2).

Decytospolide A (**18**) was isolated as an optically active colorless oil. Its molecular formula $C_{14}H_{26}O_3$ was established by HRESIMS. The absence of the ester carbonyl signal in the ^{13}C NMR spectrum suggested a different structure than that of the above lactones (Table 6). Analysis of $^1H-^1H$ COSY data

Table 6. NMR Data for Decytospolides A and B (18 and 19)[a]

	18		19	
no.	δ_H, m, *J* (Hz)	δ_C, m	δ_H, m, *J* (Hz)	δ_C, m
2	2.49, m	37.1, CH_2	2.48, m	37.2, CH_2
3		210.0, C		209.9, C
4a	2.66; dd, 15.0, 7.8;	48.4, CH_2	2.68; dd, 15.2, 7.9;	48.2, CH_2
4b	2.39, dd, 15.0, 4.8		2.38, dd, 15.2, 4.2	
5	3.74, m	74.1, CH	3.77, m	74.2, CH
6α	1.38, m	31.3, CH_2	1.40, m	30.8, CH_2
6β	1.78, m		1.75, m	
7α	2.08, m	32.9, CH_2	2.14, m	29.4, CH_2
7β	1.46, m		1.45, m	
8	3.26, dt, 10.2, 4.8	70.5, CH	4.45, dt, 10.0, 4.6	72.1, CH
9	3.04, dt, 9.0, 2.4	82.1, CH	3.23, dt, 9.3, 2.4	79.3, CH
10a	1.79, m	31.9, CH_2	1.51, m	31.9, CH_2
10b	1.36, m		1.32, m	
11a	1.47, m	25.0, CH_2	1.40, m	24.8, CH_2
11b	1.29, m		1.25, m	
12a	1.30, m	31.8, CH_2	1.25, m	31.7, CH_2
12b	1.30, m		1.25, m	
13a	1.30, m	22.6, CH_2	1.28, m	22.6, CH_2
13b	1.30, m		1.28, m	
14	0.89, t, 6.9	14.0, CH_3	0.87, t, 6.8	14.0, CH_3
15	1.05, t, 7.2	7.5, CH_3	1.04, t, 7.3	7.5, CH_3
8-OAc			2.04, s	170.3, C
				21.2, CH_3

[a]In $CDCl_3$, assignments made by DEPT, $^1H-^1H$ COSY, HSQC, HMBC and NOESY.

revealed two proton spin systems, i.e., H_3-15 to H_2-2, and H_2-4 to H_3-14. The HMBC correlation from protons H_2-2 and H_2-4 to C-3 led the connection of the two proton sequence through a ketone carbonyl. The formation of a pyran ring was apparent due to the diagnostic long-range correlation from H-5 to C-9, giving the planar structure of **18** (Figure 11). The C-5 and C-9 substituents of the furan ring had *cis* orientation, since a NOE effect was observed between the 1,3-diaxial protons of H-5 and H-9. H-8 had *trans*-diaxial relationship with H-9 due to the large coupling constant ($^3J_{H8,H9}$ = 10.2 Hz) and showed a NOE effect with H-10b (δ_H = 1.36) (see the Supporting Information, Figure S11) allowing the assignment of the relative configuration. The absolute configuration of the secondary

dx.doi.org/10.1021/jo201755v | J. Org. Chem. 2011, 76, 9699–9710

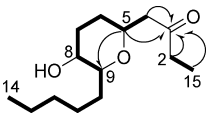

Figure 11. $^{1}H-^{1}H$ COSY (bond) and selected HMBC (arrow) correlations of **18**.

8-OH was determined as (8*S*) by the modified Mosher's method (see Supporting Information, Figure S12),[46−49] which in the knowledge of the relative configuration afforded the absolute configuration of **18** as (5*R*,8*S*,9*R*).

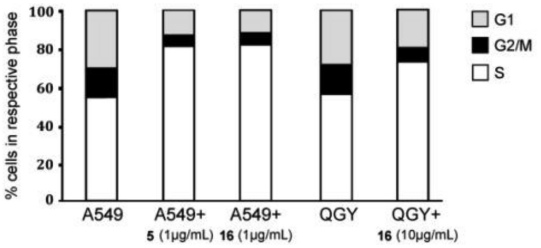

Figure 12. Effect of cytospolides E and Q (**5**, **16**) on cell cycle in A549 and QGY cells. Data were obtained by densitometry measurements (n = 3).

Decytospolide B (**19**) was isolated as an optically active colorless oil. ^{1}H and ^{13}C NMR spectra greatly resembled those of **18** except for the presence of an additional acetyl group (δ_H = 2.04, s; δ_C = 170.3, s and 21.2, q). This conclusion was in agreement with its molecular formula of $C_{16}H_{28}O_4$ as deduced from HRESIMS, showing 42 mass units more than **18**. The location of the acetyl group at C-8 was assured by the typical downfield shift of the H-8 (δ_H = 4.45 in **19** and 3.26 in **18**) (Table 6). The long-range correlation from H-8 to the acetyl carbonyl atom (δ_C = 170.3) in the HMBC spectrum further confirmed the proposed structure. The acetylation product of **18** was identical with **19**, which served as further evidence for the elucidation of the planar structure and the absolute stereochemistry. Compound **19** was thus determined as the 8-acetate derivative of **18**.

The discovery of an array of new nonanolides demonstrates the productivity of the fungus and it is an example of chemical diversity, extending the nonanolide family by derivatives formed by ring cleavage, oxidation, esterification and Michael addition. Cytospolides A−L (**1**−**12**) may biogenetically derive from precursor **A** by a dehydration involving the 5-OH, followed by oxidation at C-8, C-13, and/or C-14. Further oxidation of OH-3 would result in the reactive α,β-unsaturated ketone precursor B, the C-3 carbonyl and $\Delta^{4,5}$ bond of which can be found separately in the reported nanolides. An intermolecular Michael addition to the β carbon of the α,β-unsaturated ketone and the acetylation of 5-OH may produce cytospolide P (**16**) from precursor **B**, while an intramolecular oxa-Michael addition of 8-OH to the α,β-unsaturated ketone of precursor **B** may give cytospolide O (**15**). The subsequent oxidation of C-4 and reduction of C-3 carbonyl of cytospolide O (**15**) may produce cytospolides M and N (**13**, **14**). Consequently, a transesterification of the lactone acyl group with 4-OH of cytospolide M (**13**) would construct the γ-lactone moiety of cytospolide Q (**17**). The two decytospolides A and B (**18**, **19**) may be produced from precursor **B** by an initiation of a ring cleavage on the lactone bond, followed by intramolecular oxa-Michael addition of 9-OH to the α,β-unsaturated ketone and decarboxylation of the β-keto carboxylic acid derivative (Scheme 1).

The cytotoxic activity of compounds **6**−**19** toward the tumor cell lines of A549, HCT116, QGY, A375, and U973 was evaluated in vitro (Table 7). It had been reported that the absolute configuration of C-2 has an effect on the cytotoxic activity; e.g. cytospolide D (**4**) with (2*R*) configuration showed no activity against A-549 cell line at 50 μg/mL, while its C-2 epimer, cytospolide E (**5**), displayed modest cytotoxic activity with an IC_{50} value of 7.09 μg/mL.[46] In accordance, **16** with (2*S*) configuration showed the strongest activity against cell lines A-549, QGY and U973.

Furan containing nonanolides **13**, **14**, **15**, and **17** also showed considerably cytotoxic activity against A-549 cells. The free hydroxyl groups at C-3 and C-4 seem to play an important role for the cytotoxicity, since the inhibition remarkably decreased in compound **15** lacking the two secondary hydroxyl

Scheme 1. Proposed Biogenetic Connection of Isolated Cytospolides A−Q (1−17) and Decytospolides A and B (18 and 19)

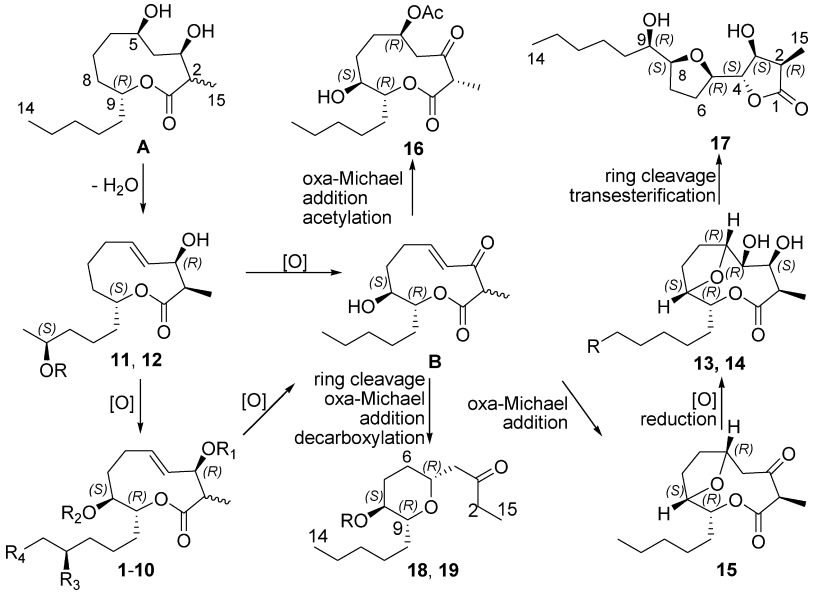

dx.doi.org/10.1021/jo201755v | *J. Org. Chem.* 2011, 76, 9699−9710

Table 7. Cytotoxic Assays toward Different Tumor Cell Lines[a,b]

no.	A549	HCT116	QGY	A375	U937
6	–	–	–	–	–
7	–	–	–	–	–
8	–	–	–	–	–
9	–	–	–	–	–
10	–	–	–	–	–
11	20.47	–	–	–	–
12	–	–	–	–	–
13	12.29	–	–	–	–
14	16.55	–	–	–	–
15	39.17	–	–	–	–
16	2.05	–	15.82	–	28.26
17	10.55	–	–	–	–
18	–	–	–	–	–
19	14.79	–	46.79	–	–
adriamycin	0.44	0.45	0.28	0.44	0.23

[a] IC_{50} (μg/mL). [b] –: IC_{50} > 50 μg/mL.

groups. The activity of decytospolide A (**18**) increased dramatically when the 8-OH was acetylated.

A cell cycle analysis was executed to further evaluate the tumor cell growth inhibition of the two potent compounds, cytospolides E and Q (**5**, **16**), both having (2*S*) absolute configuration. Both compounds can significantly mediate G1 arrest in A549 tumor cells at 1 μg/mL. The percentage of cells at the G1 phase was increased from 58.8% to 82.5% and 83.1% ($P < 0.01$), while those at the S phase were decreased from 30.3% to 11.6% and 10.2% ($P < 0.01$), respectively. Cytospolide E (**5**) was not active toward QGY cells, whereas cytospolide P (**16**) displayed a significant effect (10 μg/mL), increasing the percentage at G1 phase from 56.9% to 72.0% ($P < 0.01$) and decreasing the percentage of cells at S phase from 30.3% to 11.6% ($P < 0.01$), respectively (Figure 12).

EXPERIMENTAL SECTION

General Experimental Procedures. Precoated silica gel plates were used for analytical thin-layer chromatography (TLC). Spots were detected on TLC under UV or by heating after spraying with 0.5 mL of anisaldehyde in 50 mL of HOAc and 1 mL of H_2SO_4. TLC R_f values are reported. The NMR spectra were recorded at 293K. Chemical shifts are reported in parts per million (δ), using the residual $CHCl_3$ signal (δ_H 7.26 ppm) as an internal standard for ^{1}H NMR, and $CDCl_3$ (δ_C 77.0 ppm) for ^{13}C NMR; coupling constant (J) in Hz. ^{1}H and ^{13}C NMR assignments were supported by ^{1}H–^{1}H COSY, HMQC, HMBC, and NOESY experiments. $^3J_{C,H}$ couplings were measured by means of pulsed field gradient HMBC spectra, recorded by varying J-refocusing time τ between 0.04 and 0.16 s (10 ms interval), corresponding to $J = 1/(2\tau) = 3.1–12.5$ Hz. $^3J_{C,H}$ values were estimated with least-squares sinusoidal fit of the experimental cross-peak intensities as a function of J.[54] The following abbreviations are used to describe spin multiplicity: s = singlet, d = doublet, t = triplet, q = quartet, m = multiplet, brs = broad singlet, dd = doublet of doublets, ddd = doublet of doublets of doublets, dt = doublet of triplets, qd = quartet of doublets, ov = overlapped signals. Infrared spectra were recorded in thin polymer films. For the protocol of the solid-state circular dichroism (CD) protocol, see ref50. The mass spectra and high-resolution mass spectra were performed on a Q-TOF Micro mass spectrometer, resolution 5000. An isopropyl alcohol solution of sodium iodide (2 mg/mL) was used as a reference compound. The X-ray diffraction study was carried out using Cu Kα radiation (λ = 1.542178 Å). Semi-preparative RP-HPLC was performed using a refractive index detector and a column with 5 μm, 250 × 10 mm size.

Culture, Extraction, and Isolation. The endophytic fungus *Cytospora* sp., internal strain No. ZW02, was isolated following surface sterilization from *Ilex canariensis*, a woody, evergreen shrub from Gomera, and was cultivated on biomalt (5% w/v) solid agar medium at room temperature for 28 days.[43−45] The culture medium was then extracted with acetone to afford a residue (9.98 g) after removal of the solvent under reduced pressure. The extract was subjected to column chromatography (CC) on silica gel, eluted with a gradient of CH_2Cl_2 in acetone (100:1, 80:20, 50:50, 30:70, 1:100 v/v), to give 17 subfractions. Fractions 3 and 4 were first purified on silica gel CC (400-500 mesh, CH_2Cl_2/acetone, 100:1) and then fractionated by semi-preparative RP-HPLC (MeOH/H_2O, 8:2, 1.5 mL/min) to give **16** (1.7 mg, 15.8 min, yield 0.17‰), **15** (6.3 mg, 20.3 min, yield 2.03‰), and **19** (1.5 mg, 27.4 min, yield 2.74‰), respectively. Fractions 8−10 were first purified on silica gel CC (400-500 mesh, $CHCl_3$/MeOH, 50:1), followed by a purification of semi-preparative RP-HPLC: fraction 8 afforded **12** (1.7 mg, yield 0.17‰) at 27.7 min with the elution of MeOH/H_2O (8:2, 1.0 mL/min); fractions 9 and 10 yielded pure **7** (5.4 mg, yield 0.54‰), **13** (9.4 mg, yield 0.94‰), **14** (1.0 mg, yield 0.10‰), and **18** (8.1 mg, yield 0.81‰) at 23.2, 18.3, 19.9, and 29.7 min, respectively, eluted with MeOH/H_2O (7:3, 1.5 mL/min). Fraction 11 gave **6** (7.7 mg, yield 0.77‰) and **8** (0.9 mg, yield 0.09‰) by a simple fractionation on silica gel CC (400-500 mesh, $CHCl_3$/MeOH, 30:1). Fractions 14, 15, and 16 were purified on silica gel CC (400-500 mesh, $CHCl_3$/MeOH, 20:1), and then separated by semi-preparative HPLC, eluted with MeOH/H_2O (7:3, 1.5 mL/min) to yield pure **11** (6.6 mg, yield 0.66‰), **17** (4.5 mg, yield 0.45‰) and the mixture products **9**/**10** (6.1 mg, yield 0.61‰), at 19.6, 18.6, and 14.9 min, respectively.

Cytospolide F (6): colorless oil; R_f = 0.38 ($CHCl_3$/MeOH 10:1); $[\alpha]^{20}_D$ = −72.7 (*c* 0.08, $CHCl_3$); CD (CH_3CN, *c* 2.0 × 10^{-4}) λ_{max} ($\Delta\varepsilon$) = 195 (−11.48) nm; UV (CH_3CN) λ_{max} (ε) 219 (2449) nm; IR (film) ν_{max} = 3415, 3004, 2920, 1716, 1656, 1436, 1410, 1317, 1185, 1022, 953, 903, 707 cm^{-1}; ^{1}H and ^{13}C NMR spectroscopic data, see Tables 1 and 2; HRMS (ESI) $[M + Na]^+$ *m*/*z* 309.1675 (calcd for $C_{15}H_{26}O_5Na$, 309.1678).

Cytospolide G (7:). colorless oil; R_f = 0.79 ($CHCl_3$/MeOH 10:1); $[\alpha]^{20}_D$ = −53.7 (*c* 0.05, $CHCl_3$); UV (CH_3CN) λ_{max} (ε) 221 (1797) nm; IR (film) ν_{max} = 3406, 2930, 2857, 1737, 1670, 1457, 1375, 1240, 1180, 1106, 1065, 1024, 990, 943 cm^{-1}; ^{1}H and ^{13}C NMR spectroscopic data, see Tables 1 and 2; HRMS (ESI) $[M + Na]^+$ *m*/*z* 351.1785 (calcd for $C_{17}H_{28}O_6Na$, 351.1784).

Cytospolide H (8): colorless oil; R_f = 0.32 ($CHCl_3$/MeOH 10:1); $[\alpha]^{20}_D$ = −88.9 (*c* 0.01, $CHCl_3$); UV (CH_3CN) λ_{max} (ε) 215 (1829) nm; IR (film) ν_{max} = 3454, 3360, 3197, 2924, 2853, 1736, 1662, 1462, 1440, 1375, 1242, 1176, 1107, 1065, 1023, 989 cm^{-1}; ^{1}H and ^{13}C NMR spectroscopic data, see Tables 1 and 2; HRMS (ESI) $[M + Na]^+$ *m*/*z* 393.1887 (calcd for $C_{19}H_{30}O_7Na$, 393.1889).

Cytospolide I and J (9 and 10): colorless oil; R_f = 0.31 ($CHCl_3$/MeOH 5:1); $[\alpha]^{20}_D$ = −80.3 (*c* 0.06, $CHCl_3$); CD (CH_3CN, *c* 2.0 × 10^{-4}) λ_{max} ($\Delta\varepsilon$) = 196 (−15.16) nm; UV (CH_3CN) λ_{max} (ε) 220 (2413) nm; IR (film) ν_{max} = 3443, 2929, 2855, 1728, 1668, 1453, 1373, 1247, 1177, 1101, 1068, 1043, 989 cm^{-1}; ^{1}H and ^{13}C NMR spectroscopic data, see Tables 1 and 2; ESIMS $[M + Na]^+$ *m*/*z* 351.13.

Cytospolide K (11): colorless oil; R_f = 0.41 ($CHCl_3$/MeOH 5:1); $[\alpha]^{20}_D$ = −40.9 (*c* 0.07, $CHCl_3$); CD (CH_3CN, *c* 2.2 × 10^{-4}) λ_{max} ($\Delta\varepsilon$) = 195 (−10.90) nm; UV (CH_3CN) λ_{max} (ε) 221 (1110) nm; IR (film) ν_{max} = 3429, 2927, 2856, 1714, 1455, 1375, 1242, 1181, 1101, 1029, 979, 916 cm^{-1}; ^{1}H and ^{13}C NMR spectroscopic data, see Table 3; HRMS (ESI) $[M + Na]^+$ *m*/*z* 293.1727 (calcd for $C_{15}H_{26}O_4Na$, 293.1729).

Cytospolide L (12): colorless oil; R_f = 0.50 ($CHCl_3$/MeOH 10:1); $[\alpha]^{20}_D$ = −75.0 (*c* 0.01, $CHCl_3$); CD (CH_3CN, *c* 2.0 × 10^{-4}) λ_{max} ($\Delta\varepsilon$) = 196 (−14.48) nm; UV (CH_3CN) λ_{max} (ε) 219 (1133) nm; IR (film) ν_{max} = 3358, 3196, 2924, 2853, 1731, 1660, 1633, 1463, 1374, 1245, 1177, 1135, 1099 cm^{-1}; ^{1}H and ^{13}C NMR spectroscopic data, see Table 3; HRMS (ESI) $[M + Na]^+$ *m*/*z* 335.1831 (calcd for $C_{17}H_{28}O_5Na$, 335.1834).

Cytospolide M (13): colorless crystals (ethyl acetate/petroleum ether 2:1); mp 136−137 °C; R_f = 0.57 ($CHCl_3$/MeOH 10:1);

dx.doi.org/10.1021/jo201755v | J. Org. Chem. 2011, 76, 9699–9710

$[\alpha]^{20}_D$ = −25.5 (*c* 0.09, $CHCl_3$); CD (CH_3CN, *c* 5.0 × 10^{-4}) λ_{max} ($\Delta\varepsilon$) = 190 (+2.35), 214 (−3.07) nm; CD (KCl) λ (mdeg) 155 μg of **13** in 250 mg KCl 215 (−26.06), positive below 196 nm; UV (CH_3CN) λ_{max} (ε) 219 (1828) nm; IR (film) ν_{max} = 3346, 2928, 2856, 1731, 1665, 1459, 1377, 1184, 1131, 1098, 1064, 992, 934 cm^{-1}; ^1H and ^{13}C NMR spectroscopic data, see Table 4; HRMS (ESI) $[M + Na]^+$ *m*/*z* 309.1677 (calcd for $C_{15}H_{26}O_5Na$, 309.1678).

Cytospolide N (14): colorless oil; R_f = 0.71 ($CHCl_3$/MeOH 10:1); $[\alpha]^{20}_D$ = −60.0 (*c* 0.01, $CHCl_3$); CD (CH_3CN, *c* 5.0 × 10^{-4}) λ_{max} ($\Delta\varepsilon$) = 207 (−3.01) nm; UV (CH_3CN) λ_{max} (ε) 214 (1130) nm; IR (film) ν_{max} = 3359, 3205, 2925, 2854, 1733, 1661, 1633, 1462, 1371, 1241, 1179, 1099, 1059, 1028, 989, 935 cm^{-1}; ^1H and ^{13}C NMR spectroscopic data, see Table 4; HRMS (ESI) $[M + Na]^+$ *m*/*z* 367.1732 (calcd for $C_{17}H_{28}O_7Na$, 367.1733).

Cytospolide O (15): colorless oil; R_f = 0.47 (CH_2Cl_2/*n*-hexane 20:1); $[\alpha]^{20}_D$ = −6.3 (*c* 0.06, $CHCl_3$); CD (CH_3CN, *c* 5.0 × 10^{-4}) λ_{max} ($\Delta\varepsilon$) = 189 (−6.63), 216 (−1.83), 296 (+1.14) nm; UV (CH_3CN) λ_{max} (ε) 226 (2569), 251 (390), 278 (707) nm; IR (film) ν_{max} = 3359, 3194, 2922, 2852, 1658, 1633, 1465, 1416 cm^{-1}; ^1H and ^{13}C NMR spectroscopic data, see Table 5; HRMS (ESI) $[M + Na]^+$ *m*/*z* 291.1570 (calcd for $C_{15}H_{24}O_4Na$, 291.1572).

Cytospolide P (16): Colorless crystals (ethyl acetate/petroleum ether 2:1); mp 103−104 °C; R_f = 0.42 ($CHCl_3$); $[\alpha]^{20}_D$ = −105.9 (*c* 0.02, $CHCl_3$); CD (CH_3CN, *c* 1.0 × 10^{-3}) λ_{max} ($\Delta\varepsilon$) =198 (−1.94), 213 (−1.57), 290 (−0.88) nm; CD (KCl) λ (mdeg) 123 μg of **16** in 250 mg KCl 289 (−16.61), 214 (−21.93); UV (CH_3CN) λ_{max} (ε) 223 (2558) nm; IR (film) ν_{max} = 3408, 2926, 2855, 1736, 1708, 1669, 1459, 1372, 1242, 1073, 1030, 987, 953, 890 cm^{-1}; ^1H and ^{13}C NMR spectroscopic data, see Table 5; HRMS (ESI) $[M + Na]^+$ *m*/*z* 351.1787 (calcd for $C_{17}H_{28}O_6Na$, 351.1784).

Cytospolide Q (17): colorless crystals (CH_2Cl_2/petroleum ether 1:1); mp 97−98 °C; R_f = 0.35 ($CHCl_3$/MeOH 5:1); $[\alpha]^{20}_D$ = −4.4 (*c* 0.04, $CHCl_3$); CD (CH_3CN, *c* 8.0 × 10^{-4}) λ_{max} ($\Delta\varepsilon$) = 194 (−0.86), 217 (−1.48) nm; UV (CH_3CN) λ_{max} (ε) 219 (1537) nm; IR (film) ν_{max} = 3435, 3359, 2925, 2855, 1768, 1667, 1460, 1377, 1178, 1047,1023, 985 cm^{-1}; ^1H and ^{13}C NMR spectroscopic data, see Table 4; HRMS (ESI) $[M + Na]^+$ *m*/*z* 309.1677 (calcd for $C_{15}H_{26}O_5Na$, 309.1678).

Decytospolide A (18): Colorless oil; R_f = 0.48 ($CHCl_3$/MeOH 10:1); $[\alpha]^{20}_D$ = +6.1 (*c* 0.08, $CHCl_3$); UV (CH_3CN) λ_{max} (ε) 220 (823) nm; IR (film) ν_{max} = 3431, 2929, 2857, 1713, 1671, 1459, 1374, 1238, 1078, 1026, 989, 935 cm^{-1}; ^1H and ^{13}C NMR spectroscopic data, see Table 6; HRMS (ESI) $[M + Na]^+$ *m*/*z* 265.1778 (calcd for $C_{14}H_{26}O_3Na$, 265.1780).

Decytospolide B (19:). colorless oil; R_f = 0.51 (CH_2Cl_2/*n*-hexane 20:1); $[\alpha]^{20}_D$ = +26.6 (*c* 0.02, $CHCl_3$); UV (CH_3CN) λ_{max} (ε) 222 (2210), 267 (543), 276 (559) nm; IR (film) ν_{max} = 3360, 3193, 2923, 2852, 1658, 1633, 1465, 1416, 1315, 1235, 1134, 1043, 879 cm^{-1}; ^1H and ^{13}C NMR spectroscopic data, see Table 6; HRMS (ESI) $[M + Na]^+$ *m*/*z* 307.1888 (calcd for $C_{16}H_{28}O_4Na$, 307.1885).

X-ray Crystallographic Studies of Cytospolide M (13). A colorless needle crystal of **13** (0.05 × 0.10 × 0.10 mm) was obtained by recrystallization from ethyl acetate/petroleum ether 2:1. $C_{15}H_{26}O_5$ (M_r = 286.36), orthorhombic, space group $P2_12_12_1$ with *a* = 5.3240(1) Å, *b* = 12.6918(3) Å, *c* = 23.0937(6) Å, $\alpha = \beta = \gamma = 90.00°$, *V* = 1560.47(6) $Å^3$, *Z* = 4, D_{calcd} = 1.219 g/cm^3. Intensity data were measured using a Cu Kα radiation (graphite monochromator). A total of 4890 reflections were collected to a maximum 2θ value of 134.80° at 296 (2) K. The structure was solved by direct methods and refined by full matrix least-squares procedure. All non-hydrogen atoms were given anisotropic thermal parameters; hydrogen atoms were located from difference Fourier maps and refined at idealized positions riding on their parent atoms. The refinement converged at R1($I > 2\sigma(I)$) = 0.0568, wR2 = 0.1510 for 2552 independent reflections and 182 variables. CCDC-838718 (**13**) contains the supplementary crystallographic data for this paper. These data can be obtained free of charge from the Cambridge Crystallographic Data Centre via www.ccdc.cam.ac.uk/data_request/cif.

X-ray Crystallographic Studies of Cytospolide P (16). A colorless needle crystal of **16** (0.10 × 0.10 × 0.15 mm) was obtained by recrystallization from ethyl acetate/petroleum ether 2:1. $C_{17}H_{28}O_6$ (M_r = 328.39), orthorhombic, space group $C222_1$ with *a* = 5.1842(1) Å, *b* = 22.7750(4) Å, *c* = 30.4741(4) Å, $\alpha = \beta = \gamma = 90.00°$, *V* = 3598.08(11) $Å^3$, *Z* = 8, D_{calcd} = 1.212 g/cm^3. Intensity data were measured using a Cu Kα radiation (graphite monochromator). A total of 6130 reflections were collected to a maximum 2θ value of 134.92° at 296 (2) K. The structure was solved by direct methods and refined by full matrix least-squares procedure. All non-hydrogen atoms were given anisotropic thermal parameters; hydrogen atoms were located from difference Fourier maps and refined at idealized positions riding on their parent atoms. The refinement converged at R1($I > 2\sigma(I)$) = 0.0388, wR2 = 0.1035 for 2894 independent reflections and 210 variables. CCDC-838719 (**16**) contains the supplementary crystallographic data for this paper. These data can be obtained free of charge from the Cambridge Crystallographic Data Centre via www.ccdc.cam.ac.uk/data_request/cif.

X-ray Crystallographic Studies of Cytospolide Q (17). A colorless needle crystal of **17** (0.10 × 0.10 × 0.12 mm) was obtained by recrystallization from CH_2Cl_2/petroleum ether (1:1). $C_{15}H_{26}O_5$ (M_r = 286.36), orthorhombic, space group $P2_12_12_1$ with *a* = 5.1139(2) Å, *b* = 16.2267(5) Å, *c* = 19.0927(6) Å, $\alpha = \beta = \gamma = 90.00°$, *V* = 1584.35(9) $Å^3$, *Z* = 4, D_{calcd} = 1.201 g/cm^3. Intensity data were measured using a Cu Kα radiation (graphite monochromator). A total of 4500 reflections were collected to a maximum 2θ value of 132.02° at 296(2) K. The structure was solved by direct methods and refined by full matrix least-squares procedure. All non-hydrogen atoms were given anisotropic thermal parameters; hydrogen atoms were located from difference Fourier maps and refined at idealized positions riding on their parent atoms. The refinement converged at R1($I > 2\sigma(I)$) = 0.0311, wR2 = 0.10877 for 2571 independent reflections and 185 variables. Absolute structure parameter 0.1(2). CCDC-838720 (**17**) contains the supplementary crystallographic data for this paper. These data can be obtained free of charge from the Cambridge Crystallographic Data Centre via www.ccdc.cam.ac.uk/data_request/cif.

Esterification of Cytospolide F (6) with (*R*)-MTPA Chloride. Treatment of **6** (0.68 mg) with (*R*)-MTPA chloride (10 μL) in dry pyridine (0.5 mL), stirring at room temperature overnight, and purification by a mini silica gel column chromatography (500 mesh, *n*-hexane/$CHCl_3$, 3:1) afforded the (*S*)-MTPA ester of **6** (1.37 mg, 62%): ^1H NMR (600 MHz, $CDCl_3$) δ = 2.73 (m, 1H, H-2), 5.57 (brs, 1H, H-3), 5.66 (dd, *J* = 16.2, 2.4 Hz, 1H, H-4), 5.40 (m, 1H, H-5), 2.14 (m, 1H, H-6α), 2.14 (m, 1H, H-6β), 1.85 (m, 1H, H-7α), 1.78 (m, 1H, H-7β), 4.93 (m, 1H, H-8), 4.88 (m, 1H, H-9), 1.32 (m, 1H, H-10a), 1.32 (m, 1H, H-10b), 1.37 (m, 1H, H-11a), 1.37 (m, 1H, H-11b), 1.46 (m, 1H, H-12a), 1.46 (m, 1H, H-12b), 5.02 (m, 1H, H-13), 1.27 (t, *J* = 6.4, 3H, H-14), 1.07 (d, *J* = 7.0, 3H, H-15).

Esterification of Cytospolide F (6) with (*S*)-MTPA Chloride: The same reaction of **6** (1.03 mg) with (*S*)-MTPA chloride (15 μL) afforded the (*R*)-MTPA ester of **6** (2.16 mg, 64%): ^1H NMR (600 MHz, $CDCl_3$) δ = 2.69 (m, 1H, H-2), 5.51 (brs, 1H, H-3), 5.62 (dd, *J* = 16.2, 2.4 Hz, 1H, H-4), 5.12 (m, 1H, H-5), 2.21 (m, 1H, H-6α), 2.21 (m, 1H, H-6β), 1.92 (m, 1H, H-7α), 1.74 (m, 1H, H-7β), 4.74 (m, 1H, H-8), 4.84 (m, 1H, H-9), 1.14 (m, 1H, H-10a), 1.14 (m, 1H, H-10b), 1.13 (m, 1H, H-11a), 1.13 (m, 1H, H-11b), 1.36 (m, 1H, H-12a), 1.36 (m, 1H, H-12b), 4.95 (m, 1H, H-13), 1.24 (t, *J* = 6.4, 3H, H-14), 1.14 (d, *J* = 7.0, 3H, H-15).

Esterification of Cytospolide H (11) with (*R*)-MTPA Chloride. Compound **11** (0.56 mg) was treated with (*R*)-MTPA chloride according to the above procedure to afford the (*S*)-MTPA ester of **11** (0.81 mg, 55%): ^1H NMR (600 MHz, $CDCl_3$): δ = 2.75 (m, 1H, H-2), 5.59 (brs, 1H, H-3), 5.63 (d, *J* = 16.3 Hz, 1H, H-4), 5.36 (m, 1H, H-5), 1.90 (m, 1H, H-6α), 2.25 (m, 1H, H-6β), 1.85 (m, 1H, H-7α), 1.42 (m, 1H, H-7β), 1.45 (m, 1H, H-8α), 1.72 (m, 1H, H-8β), 4.66 (m, 1H, H-9), 1.52 (m, 1H, H-10a), 1.52 (m, 1H, H-10b), 1.40 (m, 1H, H-11a), 1.40 (m, 1H, H-11b), 1.67 (m, 1H, H-12a), 1.67 (m, 1H, H-12b), 5.11 (m, 1H, H-13), 1.24 (t, *J* = 6.2, 3H, H-14), 1.08 (d, *J* = 6.8, 3H, H-15).

Esterification of Cytospolide H (11) with (*S*)-MTPA Chloride. The same reaction of **11** (0.45 mg) with (*S*)-MTPA chloride afforded the (*R*)-MTPA ester of **11** (0.73 mg, 62%):

^{1}H NMR (600 MHz, $CDCl_3$) δ = 2.74 (m, 1H, H-2), 5.54 (brs, 1H, H-3), 5.58 (d, J = 16.3 Hz, 1H, H-4), 5.13 (m, 1H, H-5), 1.82 (m, 1H, H-6α), 2.14 (m, 1H, H-6β), 1.72 (m, 1H, H-7α), 1.40 (m, 1H, H-7β), 1.35 (m, 1H, H-8α), 1.64 (m, 1H, H-8β), 4.56 (m, 1H, H-9), 1.47 (m, 1H, H-10a), 1.47 (m, 1H, H-10b), 1.22 (m, 1H, H-11a), 1.22 (m, 1H, H-11b), 1.61 (m, 1H, H-12a), 1.61 (m, 1H, H-12b), 5.12 (m, 1H, H-13), 1.31 (t, J = 6.2, 3H, H-14), 1.17 (d, J = 6.8, 3H, H-15).

Esterification of Cytospolide R (18) with (*R*)-MTPA Chloride. Compound **18** (0.38 mg) was treated with (*R*)-MTPA chloride according to the above procedure to afford the (*S*)-MTPA ester of **18** (0.54 mg, 75%): ^{1}H NMR (600 MHz, $CDCl_3$) δ = 1.04 (t, J = 7.3, 3H, H-1), 2.47 (m, 1H, H-2a), 2.47 (m, 1H, H-2b), 2.68 (dd, J = 15.2, 7.7 Hz, 1H, H-4a), 2.40 (dd, J = 15.2, 74.9 Hz, 1H, H-4b), 3.77 (m, 1H, H-5), 1.41 (m, 1H, H-6α), 1.78 (m, 1H, H-6β), 2.23 (m, 1H, H-7α), 1.48 (m, 1H, H-7β), 4.65 (dt, J = 10.2, 2.4 Hz, 1H, H-8), 3.30 (t, J = 9.1 Hz, 1H, H-9), 1.50 (m, 1H, H-10a), 1.32 (m, 1H, H-10b), 1.16 (m, 1H, H-11a), 1.16 (m, 1H, H-11b), 1.22 (m, 1H, H-12a), 1.22 (m, 1H, H-12b), 1.23 (m, 1H, H-13a), 1.23 (m, 1H, H-13b), 0.86 (t, J = 7.0, 3H, H-14).

Esterification of Cytospolide R (18) with (*S*)-MTPA Chloride. The same reaction of **18** (0.40 mg) with (*S*)-MTPA chloride afforded the (*R*)-MTPA ester of **18** (0.49 mg, 65%): ^{1}H NMR (600 MHz, $CDCl_3$) δ = 1.04 (t, J = 7.3, 3H, H-1), 2.47 (m, 1H, H-2a), 2.47 (m, 1H, H-2b), 2.68 (dd, J = 15.2, 7.7 Hz, 1H, H-4a), 2.40 (dd, J = 15.2, 74.9 Hz, 1H, H-4b), 3.78 (m, 1H, H-5), 1.46 (m, 1H, H-6α), 1.82 (m, 1H, H-6β), 2.28 (m, 1H, H-7α), 1.63 (m, 1H, H-7β), 4.68 (dt, J = 10.2, 2.4 Hz, 1H, H-8), 3.26 (dt, J = 9.1, 1.9 Hz, 1H, H-9), 1.30 (m, 1H, H-10a), 1.18 (m, 1H, H-10b), 1.10 (m, 1H, H-11a), 1.10 (m, 1H, H-11b), 1.20 (m, 1H, H-12a), 1.20 (m, 1H, H-12b), 1.18 (m, 1H, H-13a), 1.18 (m, 1H, H-13b), 0.83 (t, J = 7.0, 3H, H-14).

Acetylation of Cytospolide E (5). Treatment of **5** (0.7 mg) with Ac_2O, using the above procedure, afforded an acetate in quantitative yield, identical with the natural product **2**.

Synthesis of 20 by Acetylation of Cytospolide F (6). To a solution of **6** (0.5 mg) in dry pyridine (0.5 mL) was added two drops of Ac_2O. The mixture was kept at room temperature for 16 h to afford, after usual workup, **20** quantitatively as colorless oil: $[\alpha]^{20}_D$ = −84.7 (c 0.04, $CHCl_3$); ^{1}H NMR (600 MHz, $CDCl_3$) δ = 2.75 (m, 1H, H-2), 5.35 (brs, 1H, H-3), 5.64 (dd, J = 15.6, 2.4 Hz, 1H, H-4), 5.52 (ddd, J = 15.6, 6.0, 4.8 Hz, 1H, H-5), 2.20 (m, 1H, H-6α), 2.25 (m, 1H, H-6β), 1.88 (m, 1H, H-7α), 1.83 (m, 1H, H-7β), 4.73 (q, J = 7.2, 1H, H-8), 4.92 (dt, J = 7.2, 3.6, 1H, H-9), 1.52 (m, 2H, H-10a, H-10b), 1.31 (m, 2H, H-11a, H-11b), 1.28 (m, 2H, H-12a, H-12b), 4.85 (m, 1H, H-13), 1.18 (t, J = 6.8, 3H, H-14), 1.18 (t, J = 6.8, 3H, H-15), 2.14 (s, 3H, 3-OAc), 2.07 (s, 3H, 8-OAc), 2.02 (s, 3H, 13-OAc); ^{13}C NMR (150 MHz, $CDCl_3$) δ = 171.7 (s, C-1), 45.0 (d, C-2), 72.6 (d, C-3), 129.1 (d, C-4), 129.1 (d, C-5), 29.3 (t, C-6), 35.5 (t, C-7), 75.1 (d, C-8), 75.6 (d, C-9), 31.8 (t, C-10), 20.4 (t, C-11), 35.6 (t, C-12), 70.6 (t, C-13), 19.9 (q, C-14), 12.3 (q, C-15), 170.2 (s, 3-OAc), 20.9 (q, 3-OAc), 169.8 (s, 8-OAc), 21.1 (q, 8-OAc), 170.7 (s, 13-OAc), 21.3 (q, 13-OAc).

Synthesis of 20 by acetylation of cytospolide G (7). The same reaction was performed with **7** (0.7 mg) to afford an identical sample of **20** as a colorless oil in quantitative yield.

Synthesis of 20 by acetylation of cytospolide H (8). The same reaction was performed with **8** (0.4 mg) to afford an identical sample of **20** as a colorless oil in quantitative yield.

Synthesis of 21 by acetylation of cytospolide K (11). Treatment of **11** (0.7 mg) with Ac_2O according to the above procedure, afforded **21** quantitatively as a colorless oil. [α]20 D= −53.4 (c 0.02, $CHCl_3$). ^{1}H NMR (600 MHz, $CDCl_3$): δ = 2.73 (m, 1H, H-2), 5.37 (brs, 1H, H-3), 5.62 (d, J = 15.6 Hz, 1H, H-4), 5.49 (m, 1H, H-5), 2.206 (m, 1H, H-6α), 2.28 (m, 1H, H-6β), 1.88 (m, 1H, H-7α), 1.45 (m, 1H, H-7β), 1.50 (m, 1H, H-8α), 1.77 (m, 1H, H-8β), 4.70 (m, 1H, H-9), 1.55 (m, 1H, H-10a), 1.45 (m, 1H, H-10b), 1.30 (m, 2H, H-11a, H-11b), 1.50 (m, 2H, H-12a, H-12b), 4.87 (m, 1H, H-13), 1.19 (t, J = 6.6, 3H, H-14), 1.18 (t, J = 6.6, 3H, H-15), 2.14 (s, 3H, 3-OAc), 2.02 (s, 3H, 13-OAc); ^{13}C NMR (150 MHz, $CDCl_3$): δ = 174.4 (s, C-1), 45.4 (d, C-2), 73.3 (d, C-3), 129.1 (d, C-4), 129.2 (d, C-5), 32.7 (t, C-6), 28.2 (t, C-7), 33.1 (t, C-8), 75.9 (d, C-9), 35.7 (t, C-10), 21.0 (t, C-11), 35.6 (t, C-12), 70.7 (t, C-13), 19.9 (q, C-14), 12.2 (q, C-15), 170.4 (s, 3-OAc), 20.9 (q, 3-OAc), 170.8 (s, 13-OAc), 21.4 (q, 13-OAc).

Synthesis of 21 by acetylation of cytospolide L (12). The same reaction was performed with **12** (0.6 mg) to afford an identical sample of **21** as a colorless oil in quantitative yield.

Acetylation of cytospolide R (18). Treatment of **18** (0.4 mg) with Ac_2O, using the above procedure, afforded an acetate in quantitative yield, identical with the natural product **19**.

Cytotoxicity assay. The cytotoxic activity of tested compounds against human lung adenocarcinoma (A549), human colon cancer cells (HCT116), human hepatocarcinoma cells (QGY), human malignant melanoma cells (A375), and human leukemic cells (U937) was assayed by the MTT [3-(4,5-dimethylthiazol-2-yl)-2,5-diphenyltetrazolium bromide] colorimetric method.[55] Adriamycin was used as standard compound.

Cell cycle test. A549 cells were treated with compounds **5** and **16** at 1 μg/mL for 48 h, and QGY cells were treated with compound **16** at 10 μg/mL for 48 h, respectively. Then the cells were trypsinized, washed with PBS twice, and then fixed with 70% ethanol on ice overnight. The fixed cells were spun down, resuspended in PBS at 1 × 10^6 cells/mL and incubated with 50 μg/mL propidium idide (PI) and 100 μg/mL ribonuclease A (RNase A) at 4 °C for 30 min, before measured by flow cytometry. All experiments were performed in triplicate. The data were expressed as mean ± SD. The significance was expressed by using one-way analyses of variance (ANOVAs) of the SPSS 13.0 for Windows (SPSS Inc., Chicago, IL, USA), followed by Duncan post hoc tests. P values less than 0.05 were considered significant.

Computational section. Geometry optimizations [B3LYP/6-31G(d) level of theory] and TDDFT calculations were performed with Gaussian 03[56] using various functionals (B3LYP, BH&HLYP, PBE0) and TZVP basis set. CD spectra were generated as the sum of Gaussians[57] with 3000 cm^{-1} half-height width (corresponding to 12 at 200 nm), using dipole-velocity computed rotational strengths. Conformational searches were carried out by means of the Macromodel 9.7.211[58] software using Merck Molecular Force Field (MMFF) with implicit solvent model for chloroform. Boltzmann distributions were estimated from the ZPVE corrected B3LYP/6-31G(d) energies. The MOLEKEL[59] software package was used for visualization of the results.

■ ASSOCIATED CONTENT

Ⓢ Supporting Information

MS, one- and two-dimensional NMR spectra for compounds **6**−**19**, X-ray data for crystals **13**, **16**, and **17** (CIF), and atom coordinates and absolute energies of the computed structures. These material are available free of charge via the Internet at http://pubs.acs.org

■ AUTHOR INFORMATION

Corresponding Author

*E-mail: (L.L.) lilingty@126.com; (W.Z.) wenzhang1968@163.com.

■ ACKNOWLEDGMENTS

This research was financially supported by the Natural Science Foundation of China (Nos. 30873200, 41076082, 81172979), the Shanghai Pujiang Program (PJ2008), the Scientific & Technological Major Project (2009ZX09301-011). S.A. and T.K. thank the Hungarian Scientific Research Fund (OTKA, K-81701), TÁMOP 4.2.1./B-09/1/KONV-2010-0007, and National Information Infrastructure Development Institute (NIIFI 10038). We are grateful to Prof. L. Ernst and Mrs. P. H. Schulz (Technische Universität Braunschweig, Germany) and Prof. E. Hans (University of Paderborn, Germany) for the assistance with the NOEDIFF experiments. We are also indebted to

Prof. R. Riguera (Universidad de Santiago de Compostela, Spain) for his kind advice concerning the Mosher experiment.

REFERENCES

(1) Dräger, G.; Kirschning, A.; Thierickeb, R.; Zerlin., M. *Nat. Prod. Rep.* **1996**, *13*, 365−375.
(2) Naves, Y. R.; Grampoloff, A. V. *Helv. Chim. Acta* **1942**, *25*, 1500−1514.
(3) Demole, E.; Willhalm, B.; Stoll, M. *Helv. Chim. Acta* **1964**, *47*, 1152−1159.
(4) Ishida, T.; Wada, K. *J. Chem. Soc., Chem. Commun.* **1975**, 209−210.
(5) Evidente, A.; Capasso, R.; Andolfi, A.; Vurro, M.; Zonno, M. C. *Phytochemistry* **1998**, *48*, 941−945.
(6) Rivero-Cruz, J. F.; García-Aguirre, G.; Cerda-García-Rojas, C.; Mata, R. *Tetrahedron* **2000**, *56*, 5337−5344.
(7) Yuzikhin, O.; Mitina, G.; Berestetskiy, A. *J. Agric. Food Chem.* **2007**, *55*, 7707−7711.
(8) Evidente, A.; Cimmino, A.; Berestetskiy, A.; Andolfi, A.; Motta, A. *J. Nat. Prod.* **2008**, *71*, 1897−1901.
(9) Rukachaisirikul, V.; Pramjit, S.; Pakawatchai, C.; Isaka, M.; Supothina, S. *J. Nat. Prod.* **2004**, *67*, 1953−1955.
(10) Boonphong, S.; Kittakoop, P.; Isaka, M.; Pittayakhajonwut, D.; Tanticharoen, M.; Thebtaranonth, Y. *J. Nat. Prod.* **2001**, *64*, 965−967.
(11) Wu, S.; Chen, Y. W.; Shao, S. C.; Wang, L. D.; Li, Z. Y.; Yang, L. Y.; Li, S. L.; Huang, R. *J. Nat. Prod.* **2008**, *71*, 731−734.
(12) Tsuda, M.; Mugishima, T.; Komatsu, K.; Sone, T.; Tanaka, M.; Mikami, Y.; Kobayashi, J. *J. Nat. Prod.* **2003**, *66*, 412−415.
(13) Chu, M.; Mierzwa, R.; Xu, L.; He, L.; Terracciano, J.; Patel, M.; Gullo, V.; Black, T.; Zhao, W.; Chan, T.; McPhail, A. T. *J. Nat. Prod.* **2003**, *66*, 1527−1530.
(14) Bugni, T. S.; Janso, J. E.; Williamson, R. T.; Feng, X.; Bernan, V. S.; Greenstein, M.; Carter, G. T.; Maiese, W. M.; Ireland, C. M. *J. Nat. Prod.* **2004**, *67*, 1396−1399.
(15) Ratnayake, A. S.; Yoshida, W. Y.; Mooberry, S. L.; Hemscheidt, T. *Org. Lett.* **2001**, *3*, 3479−3481.
(16) Papendorf, O.; König, G. M.; Wright, A. D.; Chorus, I.; Oberemm, A. *J. Nat. Prod.* **1997**, *60*, 1298−1300.
(17) Tan, Q.; Yan, X.; Lin, X.; Huang, Y.; Zheng, Z.; Song, S.; Lu, C.; Shen, Y. *Helv. Chim. Acta* **2007**, *90*, 1811−1817.
(18) Nicoletti, R.; Lopez-Gresa, M. P.; Manzo, E.; Carella, A.; Ciavatta, M. L. *Mycopathologia* **2007**, *163*, 295−301.
(19) Ferraz, H. M. C.; Bombonato, F. I.; Longo, L. S. *Synthesis* **2007**, *21*, 3261−3285.
(20) Riatto, V. B.; Pilli, R. A.; Victor, M. M. *Tetrahedron* **2008**, *64*, 2279−2300.
(21) Ishigami, K. *Biosci. Biotechnol. Biochem.* **2009**, *73*, 971−979.
(22) Chowdhury, P. S.; Gupta, P.; Kumar, P. *Tetrahedron Lett.* **2009**, *50*, 7188−7190.
(23) Mohapatra, D. K.; Sahoo, G.; Ramesh, D. K.; Rao, J. S.; Sastry, G. N. *Tetrahedron Lett.* **2009**, *50*, 5636−5639.
(24) Krishna, P. R.; Rao, T. J. *Tetrahedron Lett.* **2010**, *51*, 4017−4019.
(25) Yadav, J. S.; Lakshmi, K. A.; Reddy, N. M.; Prasad, A. R.; Subba Reddy, B. V. *Tetrahedron* **2010**, *66*, 334−338.
(26) Gupta, P.; Kumar, P. *Tetrahedron: Asymmetry* **2007**, *18*, 1688−1692.
(27) Nagaiah, K.; Sreenu, D.; R. Rao, S.; Yadav, J. S. *Tetrahedron Lett.* **2007**, *48*, 7173−7176.
(28) Selvam, J. J. P.; Rajesh, K.; Suresh, V.; Babu, D. C.; Venkateswarlu, Y. *Tetrahedron: Asymmetry* **2009**, *20*, 1115−1119.
(29) Kamal, A.; Reddy, P. V.; Prabhakar, S. *Tetrahedron: Asymmetry* **2009**, *20*, 1120−1124.
(30) Srihari, P.; Rao, G. M.; Rao, R. S.; Yadav, J. S. *Synthesis* **2010**, 2407−2412.
(31) Chakraborty, T. K.; Samanta, R.; Kumar, P. K. *Tetrahedron* **2009**, *65*, 6925−6931.
(32) Matsuda, M.; Yamazaki, T.; Fuhshuku, K.-i.; Sugai, T. *Tetrahedron* **2007**, *63*, 8752−8760.
(33) Ghosh, S.; Rao, R. V. *Tetrahedron Lett.* **2007**, *48*, 6937−6940.
(34) Yadav, J. S.; Thrimurtulu, N.; Gayathri, K. U.; Reddy, B. V. S.; Prasad, A. R. *Tetrahedron Lett.* **2008**, *49*, 6617−6620.
(35) Barfoot, C.; Burns, A.; Edwards, M.; Kenworthy, M.; Ahmed, M.; Shanahan, S.; Taylor, R. *Org. Lett.* **2008**, *10*, 353−356.
(36) Chowdhury, P. S.; Gupta, P.; Kumar, P. *Tetrahedron Lett.* **2009**, *50*, 7018−7020.
(37) Marrero, J. G.; Harwood, L. M. *Tetrahedron Lett.* **2009**, *50*, 3574−3576.
(38) Jana, N.; Mahapatra, T.; Nanda, S. *Tetrahedron: Asymmetry* **2009**, *20*, 2622−2628.
(39) Srihari, P.; Kumaraswamy, B.; Rao, G. M.; Yadav, J. S. *Tetrahedron: Asymmetry* **2010**, *21*, 106−111.
(40) Prabhakar, P.; Rajaram, S.; Reddy, D. K.; Shekar, V.; Venkateswarlu, Y. *Tetrahedron: Asymmetry* **2010**, *21*, 216−221.
(41) Srihari, P.; Kumaraswamy, B.; Bhunia, D. C.; Yadav, J. S. *Tetrahedron Lett.* **2010**, *51*, 2903−2905.
(42) Burns, A.; McAllister, G.; Shanahan, S.; Taylor, R. *Angew. Chem., Int. Ed.* **2010**, *49*, 5574−5577.
(43) Zhang, W.; Krohn, K.; Zia-Ullah.; Flörke, U.; Pescitelli, G.; Bari, L. D.; Antus, S.; Kurtán, T.; Rheinheimer, J.; Draeger, S.; Schulz, B. *Chem.—Eur. J.* **2008**, *14*, 4913−4923.
(44) Zhang, W.; Krohn, K.; Egold, H.; Draeger, S.; Schulz, B. *Eur. J. Org. Chem.* **2008**, 4320−4328.
(45) Zhang, W.; Krohn, K.; Draeger, S.; Schulz, B. *J. Nat. Prod.* **2008**, *71*, 1078−1081.
(46) Lu, S.; Kurtán, T.; Yang, G.; Sun, P.; Mándi, A.; Krohn, K.; Draeger, S.; Schulz, B.; Yi, Y.; Li, L.; Zhang, W. *Eur. J. Org. Chem.* **2011**, 5452−5459.
(47) Dale, J. A.; Mosher, H. S. *J. Am. Chem. Soc.* **1973**, *95*, 512−519.
(48) Ohtani, I.; Kusumi, T.; Kashman, Y.; Kakisawa, H. *J. Am. Chem. Soc.* **1991**, *113*, 4092−4096.
(49) Ohtani, I.; Kusumi, T.; Kashman, Y.; Kakisawa, H. *J. Org. Chem.* **1991**, *56*, 1296−1298.
(50) Pescitelli, G.; Kurtán, T.; Flörke, U.; Krohn, K. *Chirality* **2009**, *21*, E181−201.
(51) Diedrich, C.; Grimme, S. *J. Phys. Chem. A* **2003**, *107*, 2524−2539.
(52) Crawford, T. D. *Theor. Chem. Acc.* **2006**, *115*, 227−245.
(53) Contreras, R. H.; Peralta, J. E. *Prog. Nucl. Magn. Reson. Spectrosc.* **2000**, *37*, 321−425.
(54) Bifulco, G.; Dambruoso, P.; Gomez-Paloma, L.; Riccio, R. *Chem. Rev.* **2007**, *107*, 3744−3779.
(55) Mosmann, T. *J. Immunol. Meth.* **1983**, *65*, 55−63.
(56) Frisch, M. J.; Trucks, G. W.; chlegel, H. B.; Scuseria, S G. E.; Robb, M. A.; Cheeseman, J. R.; Montgomery, J. A., Jr.; Vreven, T.; Kudin, K. N.; Burant, J. C.; Millam, J. M.; Iyengar, S. S.; Tomasi, J.; Barone, V.; Mennucci, B.; Cossi, M.; Scalmani, G.; Rega, N.; Petersson, G. A.; Nakatsuji, H.; Hada, M.; Ehara, M.; Toyota, K.; Fukuda, R.; Hasegawa, J.; Ishida, M.; Nakajima, T.; Honda, Y.; Kitao, O.; Nakai, H.; Klene, M.; Li, X.; Knox, J. E.; Hratchian, H. P.; Cross, J. B.; Bakken, V.; Adamo, C.; Jaramillo, J.; Gomperts, R.; Stratmann, R. E.; Yazyev, O.; Austin, A. J.; Cammi, R.; Pomelli, C.; Ochterski, J. W.; Ayala, P. Y.; Morokuma, K.; Voth, G. A.; Salvador, P.; Dannenberg, J. J.; Zakrzewski, V. G.; Dapprich, S.; Daniels, A. D.; Strain, M. C.; Farkas, O.; Malick, D. K.; Rabuck, A. D.; Raghavachari, K.; Foresman, J. B.; J. Ortiz, V.; Cui, Q.; Baboul, A. G.; Clifford, S.; Cioslowski, J.; Stefanov, B. B.; Liu, G.; Liashenko, A.; Piskorz, P.; Komaromi, I.; Martin, R. L.; Fox, D. J.; Keith, T.; Al-Laham, M. A.; Peng, C. Y.; Nanayakkara, A.; Challacombe, M.; Gill, P. M. W.; Johnson, B.; Chen, W.; Wong, M. W.; Gonzalez, C.; Pople, J. A. *Gaussian 03, Revision C.02*, Gaussian, Inc., Wallingford CT, 2004.
(57) Stephens, P. J.; Harada, N. *Chirality* **2010**, *22*, 229−233.
(58) MacroModel, Schrödinger LLC, 2009. http://www.schrodinger.com/Products/macromodel.html.
(59) Varetto, U. MOLEKEL 5.4., 2009, Swiss National Supercomputing Centre, Manno, Switzerland.